Astronomy
&
Astrophysics

The X-ray Luminosity Distributions of the high-metallicity open cluster Blanco 1

I. Pillitteri[1], G. Micela[2], S. Sciortino[2], and F. Favata[3]

[1] Dipartimento di Scienze Fisiche e Astronomiche, Sezione di Astronomia, Università di Palermo, Piazza del Parlamento 1, 90134 Palermo, Italy
e-mail: pilli@astropa.unipa.it

[2] INAF – Osservatorio Astronomico di Palermo, Piazza del Parlamento 1, 90134 Palermo, Italy
e-mail: giusi@astropa.unipa.it, sciorti@astropa.unipa.it

[3] Astrophysics Division, Research & Scientific Support Department of ESA, ESTEC, Postbus 299, 2200 AG Noordwijk, The Netherlands
e-mail: fabio.favata@rssd.esa.int

Abstract. We present X-ray Luminosity Distributions (XLDs) of late-type members (dF, dG, dK, dM) of the Blanco 1 cluster, based on ROSAT-HRI data and new astrometric-photometric membership obtained from the GSC-II project. For the first time we present the XLD of dM stars of this cluster. The high metallicity of Blanco 1 allows us to investigate the role of chemical composition on the coronal emission of late-type stars. Comparison between X-ray Luminosity Distributions of Blanco 1 and Pleiades, NGC 2516 and α Per suggests a possible metallicity effect in dM stars.

Key words. X-ray: stars – stars: activity – open clusters and associations: individual: Blanco 1

1. Introduction

Metal abundances can influence the X-ray emission of solar type stars in different ways. High presence of metals increases the radiative losses in the corona affecting the balance between heating, conduction and radiative losses. Furthermore, higher metallicity produces a deeper convective zone in stars of a given mass (through opacity changes in subphotospheric layers). This increases the convective turnover time leading to an enhancement of the dynamo efficiency that should produce a larger coronal emission (Jeffries et al. 1997). Metallicity can also influence the stellar rotational history, thus affecting the efficiency of magnetic braking.

In this context the study of the Blanco 1 cluster is important because of its peculiarities. In fact, Blanco 1 is a young open cluster, with an age estimated in the range 50−100 Myr (de Epstein & Epstein 1985; Westerlund et al. 1988; Edvardsson et al. 1995; Panagi & O'Dell 1997), a metallicity higher than the solar one ([Fe/H] $\sim$ +0.23, Edvardsson et al. 1995) and also peculiar is its location out of the galactic plane ($b = -79°$) at a distance of ~250 pc from the Sun. In the following we will assume that the age of Blanco 1 is 100 Myr in agreement with Panagi & O'Dell (1997). The temperature scale adopted by Edvardsson et al. (1995) to derive the metallicity of Blanco 1 is different from that used in studying other clusters like the Pleiades (see Boesgaard & Friel 1990). As pointed out by Jeffries & James (1999), when using the same scale adopted

for Pleiades, the metallicity value of Blanco 1 should be reduced to +0.14, a value still higher than the solar one.

Previous membership studies have been largely based on photometric criteria (Epstein 1968; de Epstein & Epstein 1985; Westerlund et al. 1988; Panagi & O'Dell 1997). To date, the most complete published member list is due to Panagi & O'Dell (1997). This list does not include dM stars. Membership lists for some F, G and early K stars based on stellar motions (radial velocity measurements) are presented in Jeffries & James (1999) and Edvardsson et al. (1995) comprising a total of ~40 objects.

The X-ray properties of Blanco 1 have been investigated by Micela et al. (1999a; hereafter Paper I). The authors have analysed the data obtained from two ROSAT-HRI observations for a total of ~160 ksec, calculated the X-ray Luminosity Distributions (XLDs) for the dG and dK stars of the cluster, adopting the photometric member list of Panagi & O'Dell (1997), and compared the XLDs with those of Pleiades and α Per clusters. Furthermore, a list of unidentified stellar-like sources, that were luminous in the X-ray band were reported. Micela et al. (1999a) argued that a fraction of these X-ray sources are likely to be low mass members of Blanco 1. The lack of membership information for dM stars has not allowed them to compare the coronal properties of these stars with the analogs of Pleiades and α Per and the possibility of contamination of the member list by older, less active field stars made the results somewhat uncertain for dG and dK spectral types.

Taking advantage of the new analysis of proper motions (G. Hawkins, private communication) for this cluster, based on

the GSC-II catalog data, we have derived membership probabilities and recomputed unbiased XLDs using the two ROSAT-HRI observations in Paper I, minimizing the contamination of field stars. Furthermore, we can now calculate for the first time the XLD of dM stars of Blanco 1. We will compare the Blanco 1 XLDs with the XLDs of the stars in the Pleiades, NGC 2516 and α Per, discussing the influence of age and metallicity on the X-ray emission level. These comparison clusters have been chosen because their properties are well known: the Pleiades cluster is ~100 Myr old and has solar metallicity (Boesgaard & Friel 1990); NGC 2516 has an age of ~100 Myr and metallicity −0.3 dex lower than the solar one (Jeffries et al. 1997); α Per is 50 Myr old and has solar metallicity (Mermilliod 1981).

The structure of our paper is as follows: in Sect. 2 we describe the method adopted for selecting members, in Sect. 3 we present the XLDs and compare them with the analogs of Pleiades, NGC 2516 and α Per discussing the implications of observed differences with respect to age and metallicity, in Sect. 4 we present our conclusions.

2. Member selection

2.1. The method

An initial sample was selected of 8069 objects with instrumental R magnitude down to ~20, extracted from the GSC-II[1] catalog and falling in the region of $1.7° \times 1.7°$ centered at RA = 00:04:08.0 (J2000) Dec = −29:57:12.6 (J2000) which contains Blanco 1. We calculated the membership probability for Blanco 1 on the basis of the following criteria:

1. Photometric selection in order to reject the objects with photometry clearly inconsistent with that of the cluster.
2. Spatial selection to keep only objects in the ROSAT-HRI fields of view of the observations analyzed in Paper I.
3. Calculation of astrometric membership probability.
4. Second photometric selection based on the cluster main sequence determined considering only the cluster high probability objects ($p \geq 0.8$) from *step* 3.
5. New astrometric membership probability for the photometric selected sample.
6. Final selection of stars with membership probability $p \geq 0.8$.

We give below a more detailed description of these steps. From the initial sample of 8069 objects (their proper motions are shown in Fig. 1) we selected 1650 objects, with both colors and magnitudes in a "strip" a few magnitudes broad that approximately mimics the cluster sequence (Fig. 2, *step* 1) in order to exclude a large fraction of faint objects not related to the cluster. Since we are working on instrumental photometry, we have not attempted to use a ZAMS model (which would require accurate color transformations) but have traced our strip by eye. All the stars confirmed as members in Jeffries & James (1999) on the basis of their radial velocity lie inside the selected strip.

[1] Details on the B and R magnitudes of the GSC-II project can be found at the web page: http://www-gsss.stsci.edu/
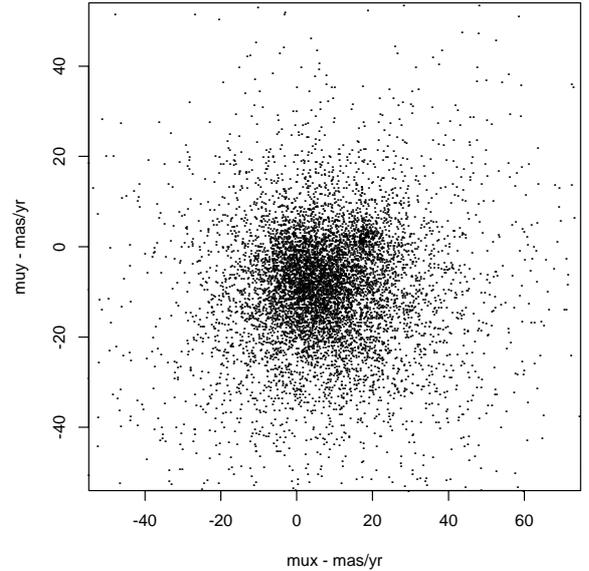

Fig. 1. Vector Point Diagram obtained from the 8069 GSC-II objects in the Blanco 1 region. The cluster is located at ~20 and 2 mas yr^{-1} along μ_x and μ_y respectively, but the contamination from field objects is clearly not negligible.
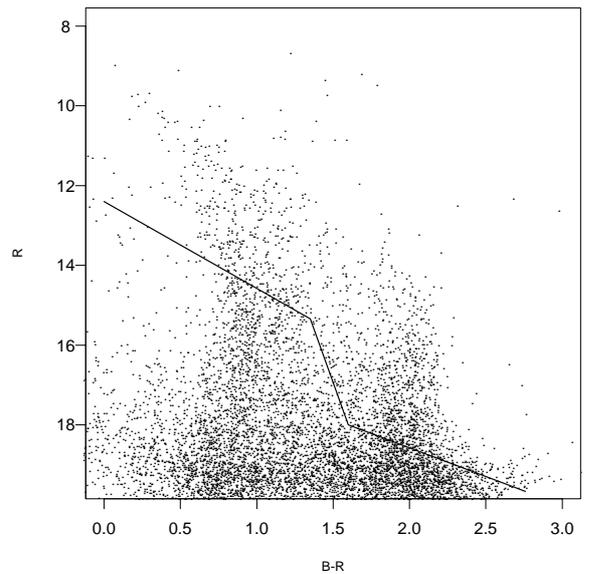

Fig. 2. R vs. $B − R$ diagram of the complete GSC-II sample. The lines show the first photometric selection based on instrumental magnitudes B and R: only the objects above the lines are retained (*step* 1).

In this phase we also rejected extended sources and those with very large astrometric errors.

Since our main interest is to reliably select cluster members in the region observed in the two ROSAT-HRI exposures, we restricted the analysis to these regions (*step* 2). We calculated the astrometric membership probability by fitting the point density in a Vector Point Diagram following the procedure described in Jones (1997) (*step* 3).

Figure 3 shows the R vs. $B − R$ scatter plot of the stars considered in this step, with open and filled squares indicating the stars with probability $p \geq 0.8$. The objects with $p \geq 0.8$ occupy two different regions; in particular the open squares clearly
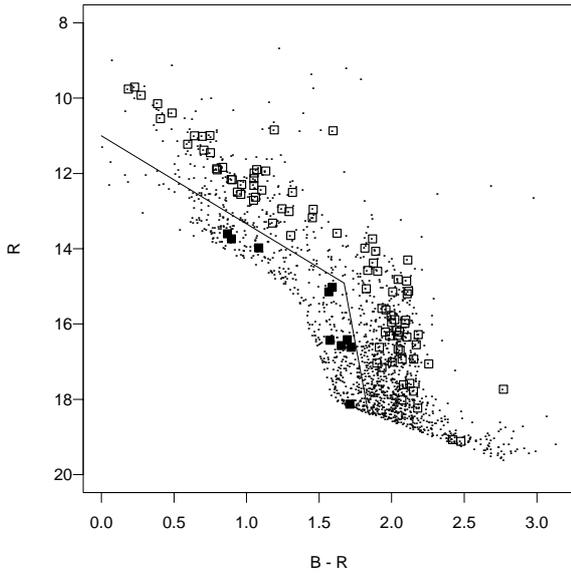
Fig. 3. R vs. $B − R$ diagram showing the second photometric selection (*step* 4) based on instrumental magnitudes B and R. Square symbols are the objects with $p \geq 0.8$ found in *step* 3. Stars shown as open squares delineate the main sequence of Blanco 1, while filled squares indicate the objects with $p \geq 0.8$ not on the same sequence. Lines show the cut leading to the new photometric selection obtained in *step* 4.
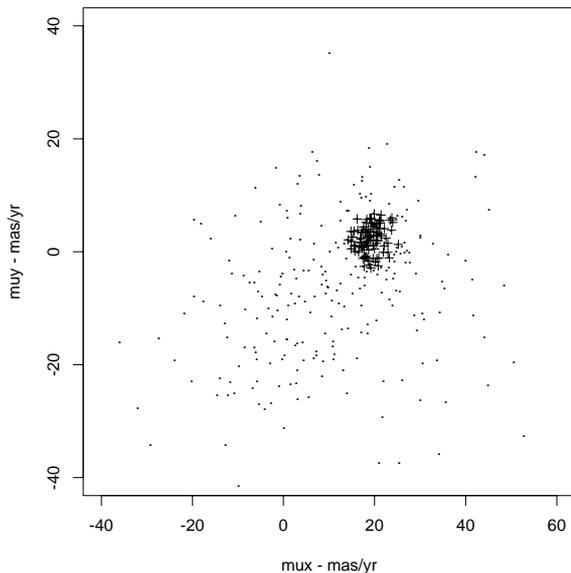

Fig. 5. Scatter plot and best fit of $B − V$ vs. $B − R$ instrumental values used to obtain the $B − V$ color index values for the Blanco 1 selected members as described in Sect. 2.1.

At the end of this procedure, we selected 93 stars as members of the cluster with proper motion probability $p \geq 0.8$ (*step* 6, Fig. 4). By integrating the values $(1 − p)$ for all the selected objects ($p \geq 0.8$) we estimated that ~9 of the 93 members are likely to be false members, thus implying a fraction of ~10% of contamination in our sample. We found that the cluster has proper motion components $\mu_\alpha \cos(\delta) = 19 \pm 4$ mas/yr and $\mu_\delta = 2 \pm 3$ mas/yr in agreement with the values derived by Robichon et al. (1999) (19.15 ± 0.50, 3.21 ± 0.27 mas/yr respectively). The values in Robichon et al. (1999) were derived from Hipparcos observations but from a sample of only 13 members of Blanco 1. We calculated the XLDs as discussed in Sect. 3 by considering a subsample of 82 members comprising only stars in the range of dF–dM type, namely 8 dF, 11 dG, 38 dK and 25 dM stars. Five out of the remaining 11 are G–M type stars just on the edge of the field of view with unreliable L_X determination, and 6 of the remaining have $B − V \leq 0.3$. The selection method, based on photometry and proper motion analysis, does not produce a bias from the point of view of X-ray emission, making it suitable to estimate Blanco 1 X-ray properties.

From the instrumental magnitude B and R we obtained a standard $B − V$ color index using conversion tables provided by G. Hawkins (private communication). These tables report measurements of $B − R$ for a sample of stars with well assessed $B − V$ index; the reliably calibration is reported in Fig. 5. We fitted a linear relation, after exclusion of some evident outliers, and calculated the index color $B − V$ from the instrumental $B − R$ values of our sample. The outliers are probably dM type stars with unreliable $B − V$ measurements. From Fig. 5 we can estimate that our fitting is reliable just to $B − R \sim 2.3$.

The fitted relation is:

$$(B − V) = (0.742 \pm 0.004)\,(B − R) − (0.035 \pm 0.004).$$

The deduced $B − V$ color index has been used to segregate the members in "spectral type" bins. In the case of dM stars,

Fig. 4. Vector Point Diagram of photometrically and spatially selected stars, crosses indicate stars with probability $p \geq 0.8$ (calculated in *step* 5).

delineate the main sequence of the cluster, while the filled squares appear outside this sequence. This behaviour prompted us to make a further cut in the initial photometric strip and to retain only the objects lying above the lines indicated in Fig. 3, thus allowing us to make the further photometric selection implemented in *step* 4. As a check, we note that this further photometric selection contains the star members in Jeffries & James (1999). We repeated the astrometric analysis (*step* 5) on the objects selected by *step* 4.
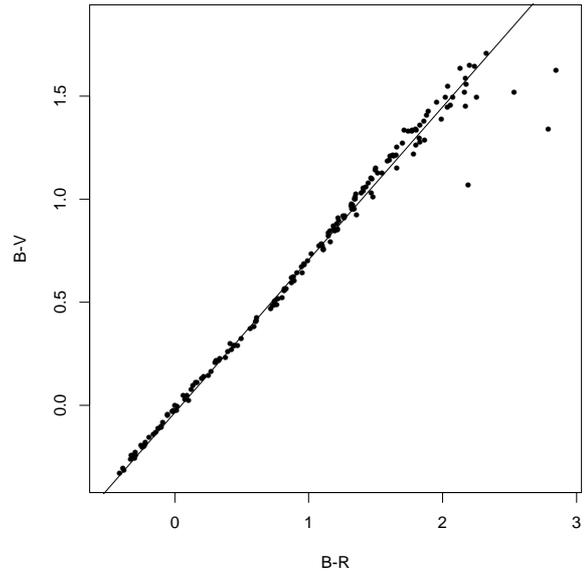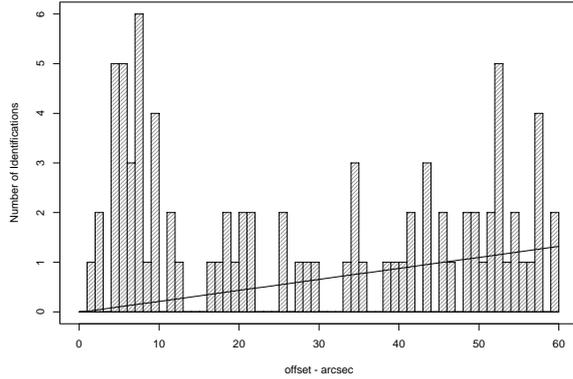
Fig. 6. Distribution of offsets between BLX sources and GSC-II stars. The line represents the distribution of expected spurious identifications.

Fig. 7. Distribution of membership probability of identified stars in the BLX list.

for which the $B - V$ index is ineffective to distinguish the various spectral sub-types, we used infrared photometry from the 2MASS catalog to assign the values of T_{eff} and spectral type. We obtained a linear relation between T_{eff} and the $H - K$ color index from the data reported in Leggett et al. (1996) and Leggett et al. (1998) and applied this relation to our sample. We found the relation:

$$T_{eff} = (4470 \pm 110) \, \text{K} - (4800 \pm 400) \text{K/mag} \, (H - K). \quad (1)$$

The typical error in the estimated temperatures is $\sim 100-150$ K, corresponding to an uncertainty of ± 1 sub-spectral type in the dM range. The temperature values from this calibration are in good agreement with those obtained from the spectral classification of a subsample of stars with low-resolution spectra ($R \sim 3000$) observed at the ESO 1.5 mt. telescope in La Silla (Chile).

2.2. X-ray member candidates

In order to identify new low-mass members among the X-ray luminous sources that were unidentified in Paper I (BLX list hereafter), we first cross-identified the positions of the BLX list with the positions of the complete sample of 8069 GSC-II objects. The positions in the BLX list are taken from Paper I, where the systematic offsets had already been removed in the ROSAT pointing solution. On the basis of the histogram shown in Fig. 6 we considered an identification correct if the offset between the position of a given X-ray source and the possible optical counterpart is $\leq 13''$ (the number of expected spurious identifications with this criterion is 1.6). We chose $13''$ as threshold for identifications on the basis of the local minimum in the distribution shown in Fig. 6. Of 88 BLX sources, 48 are identified in the GSC-II initial sample of 8069 objects, while the other 40 sources are classified as follow:

- 23 do not show GSC-II counterparts up to a distance of $20''$, i.e. the limit reported in Paper I for optical identification.
- 11 show an object at the edge of the identification circle of $20''$.
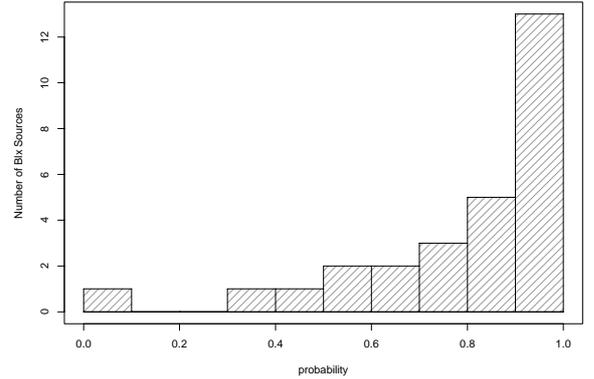- 5 show a faint object in the Digitized Sky Survey not present in the GSC-II catalog.

- 1 source is near a bright star that makes it impossible to calculate accurate positions and proper motions.

In 8 cases, the determination of the extension of GSC-II counterparts suggests that these sources are galaxies or galaxy clusters.

By adopting a radius of $13''$ we then identified again the BLX sources with the sample obtained in *steps* 5 and 6 (second and final astrometric analysis), and selected a subgroup of 28 objects. For these 28 sources the distribution of membership probability is shown in Fig. 7: 18 show a probability level higher than or equal to 80% which makes them probable low-mass members of the cluster. This conclusion is supported by spectral identification of some high probability BLX sources based on low-resolution spectra obtained at the ESO 1.5 m telescope in La Silla; these sources also show strong emission in the $H\alpha$ line (Fig. 8).

2.3. Previous photometric member list

In order to verify the field star contamination present in the list of photometric members used in previous studies, we have applied the same analysis to the members in the list of Panagi & O'Dell (1997) finding that 76 out of the 83 objects which lie in the ROSAT-HRI fields are identified with objects in the GSC-II catalog. A subsample of 68 of these 76 stars survives our selection, allowing us to assign a value of astrometric membership to this group. If we calculate the number of contaminants among these 68 stars by integrating the value $(1 - p)$ as done in Sect. 2.1, we can estimate that ~ 24 of the 68 stars are not members viz. a fraction of $\sim 35\%$. As a comparison, the fraction of contaminants in the Jeffries & James (1999) sample is $\sim 40\%$. We obtained this estimate by considering the numbers of stars from Tables 1 and 2 in Jeffries & James (1999); we also excluded 3 stars from the non-member list because these probably belong to binary systems. We conclude that the results (such as those presented in Paper I) based on the photometric list of members in Panagi & O'Dell (1997) are likely to be heavily contaminated. A mixture of age in a sample composed by Blanco 1 stars and field stars can cause significant differences in derived coronal activity, thus affecting the study of global properties that we discuss in the following.
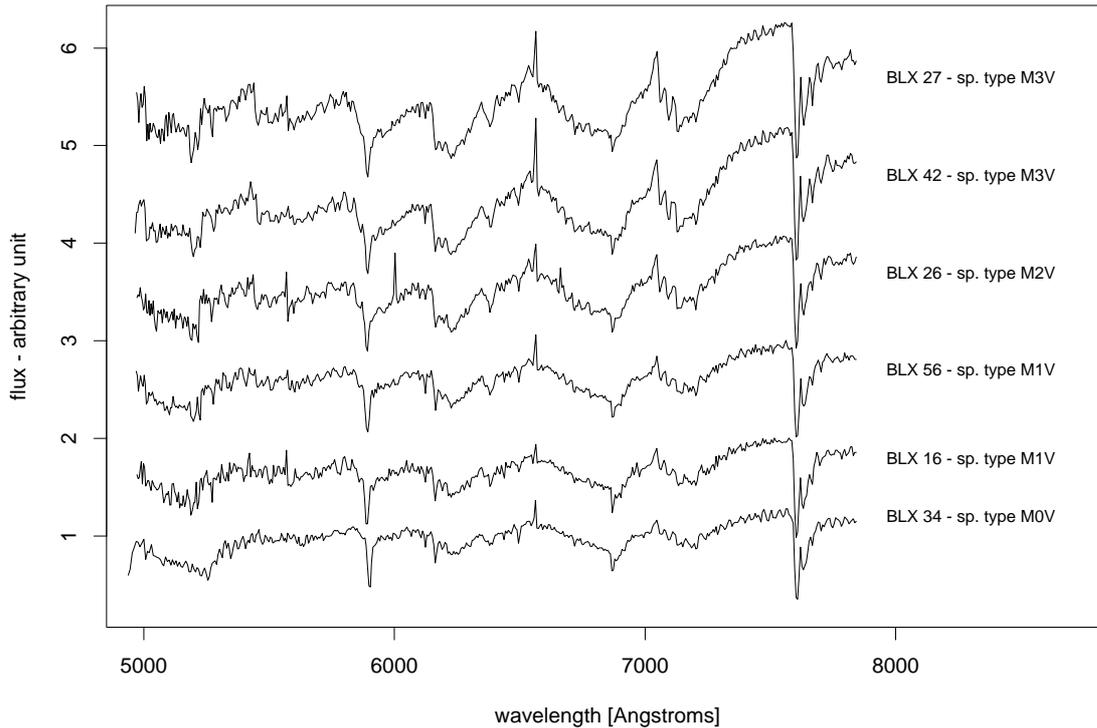
Fig. 8. Low-resolution optical spectra of the couterpart of some BLX source with membership probability $p \geq 75\%$. The flux is normalized at 5550 Å and the spectra are shifted vertically for clarity. We note in all cases the strong emission in the Hα line at 6563 Å.

3. X-ray luminosity distributions

We calculated the upper limits to the X-ray luminosity at a level corresponding to a source detection probability of 4.5 σ (consistent with the chosen detection threshold) for the undetected cluster members (i.e. stars with $p \geq 0.8$) in the HRI fields using the wavelet transform detection algorithm developed by Damiani et al. (1997). For the detections we cross-identified our optical catalog of 93 high probability members with the X-ray sources identified in Paper I, choosing the threshold radius of 13″, already used when identifying the BLX sources. This choice should minimize the loss of real identifications and the probability of chance coincidence. Coherently with the analysis carried out in Paper I, we assumed a count rate to flux conversion factor of 3.2×10^{-11} erg/(s cm^{-2} count^{-1}), derived for an optically-thin plasma model characterized by a single temperature of 1 keV (Raymond & Smith 1977) and assuming a $\log(N_{\rm H}/{\rm cm}^{-2}) = 20$, derived from $E(B-V) = 0.02$ (Westerlund et al. 1988). Uncertainties in the temperature lead to an uncertainty of 20% in the conversion factor as reported in Paper I. To calculate the X-ray luminosity, we assumed a cluster distance of 250 pc as reported in Panagi & O'Dell (1997). When using the Hipparcos distance for Blanco 1 (262 pc, Robichon et al. 1999) the X-ray luminosities should be systematically increased by ∼10%. In the appendix, Table A.1 summarizes the optical, infrared and X-ray band properties of the Blanco 1 members in the combined fields of view of the two HRI observations as well as proper motion probabilities and identifiers. Identifiers with prefix ZS are from de Epstein & Epstein (1985) while the prefix BLX refers to BLX sources from Paper I; positions are taken from the GSC-II catalog.

The $T_{\rm eff}$ values are derived using the relationship of Lang (1992) for stars with $B - V \leq 1.4$, otherwise we used Eq. (1) to assign a temperature. The mass estimates are interpolated on the values of $T_{\rm eff}$ from an isochrone model (Siess et al. 2000) calculated using metallicity $Z = 0.03$ and age 100 Myr.

The new member list contains 46 of the 83 stars from the member list given in Panagi & O'Dell (1997); for 31 of these 46 stars an X-ray detection is reported. A further 18 members not included in the Panagi & O'Dell (1997) catalog are identified with bright X-ray sources in the BLX list. We have also found a number of faint members for which we can only put an upper limit to their X-ray luminosity.

We selected dF, dG and dK type stars by the following $(B - V)_0$ ranges: 0.3–0.5, 0.5–0.8 , 0.8–1.45 respectively. For dM stars we applied the combined criteria: $B - V \geq 1.45$ and $T_{\rm eff}(H - K) < 4000$ K, using the temperature estimate from 2MASS infrared photometry. In Fig. 9 we plot $\log L_{\rm X}$ vs. $(B - V)_0$ assuming the correction $E(B - V) = 0.02$ reported by Westerlund et al. (1988), as well as the medians of $\log L_{\rm X}$ of dF, dG, dK and dM stars of Blanco 1 in the present work and, for comparison, that of the Pleiades (Micela et al. 1996 and Micela et al. 1999b). The vertical lines indicate the 10%–90% range of the distributions; in the case of dM stars the upper limit indicates that the X-ray distribution does not reach the 0.9 level because of the significant fraction of upper limits. Medians and percentile ranges are calculated by interpolating the values of $\log L_{\rm X}$ at which the XLD, as computed below, is equal to 0.5, 0.1 and 0.9 respectively. Notice that the median value of $L_{\rm X}$ for dK stars is affected by the low values for the latest types. A change of $L_{\rm X}$ at $(B - V)_0 \sim 1.4$ it is also evident. We have decided to use this color binning for consistency with the

Table 1. Numbers of detected stars in X-ray and upper limits among the Blanco 1 members.

Spectral Type	Detections	Upper Limits
dF	6	2
dG	8	3
dK	22	16
dM	10	15
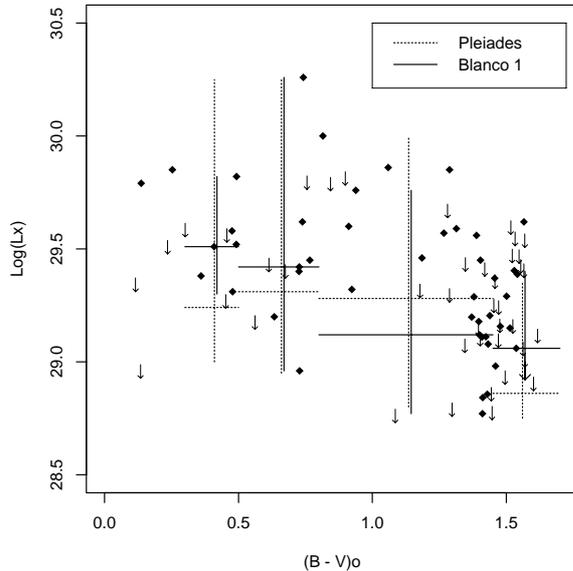
Fig. 9. $\log L_X$ vs. $B - V$ for the Blanco 1 stars. The arrows show the upper limits, the horizontal lines are the medians of distribution of $\log L_X$ in Blanco 1 (solid line) and Pleiades (dashed line), the vertical lines show the 10%−90% of distribution range.

previous work on other clusters, but it is clear that the obtained median value is strongly dependent on the chosen spectral type boundaries. Table 1 shows the number of detections and upper limits for the 82 selected Blanco 1 members. We note that the spread of Blanco 1 X-ray luminosities is comparable to that of the Pleiades regardless of the differences in metallicity, and also that the X-ray luminosity medians for dG and dK stars in Blanco 1 are lower than those of the Pleiades. In the case of dM stars, we note that the X-ray luminosity median in Blanco 1 dM stars is slightly higher than the analog for the Pleiades.

We estimate the XLDs following the method described in Schmitt (1985) in the case of censored data as done in Paper I. We do not find significant differences between XLDs computed in the present work and those in Paper I.

The median of $\log L_X$ for dG stars is now larger than that in Paper I (median $\log L_X = 29.21$ in Paper I, 29.4 in this work). In contrast, in the case of dK stars the new median is lower than that in Paper I (29.1 vs. 29.3), the reason for this unexpected difference being that we have excluded contaminants (that should lower the XLD), but have also included new late dK stars which are less active than early dK stars.

In order to investigate effects related to stellar metallicity, in Figs. 10 and 11 we compare the XLDs of dF, dG, dK and dM stars in Blanco 1, Pleiades (Micela et al. 1996; Micela et al. 1999b) and NGC 2516 (Harnden et al. 2001). The XLDs of

NGC 2516 are derived from *Chandra* data, so that the comparison with other XLDs, obtained with a different instrument, is not straightforward. Furthermore the membership information for NGC 2516 is not yet as reliable as that for the Pleiades, thus in this case the XLDs could still be affected by contamination in the range of solar type stars. However, our primary comparison relies on Blanco 1 vs. the Pleiades and α Per clusters for which we used ROSAT data and for which astrometric membership is available. We have not found any significant differences between Blanco 1 and Pleiades stars for dG and dK spectral type when applying several statistical "two sample" tests (logrank, Gehan and Wilcoxon, see Schmitt 1985); while we found a marginal difference at the 94% level in the case of dM stars[2].

The dG stars of Blanco 1 have a distribution of $\log L_X$ values similar to that of Pleiades and NGC 2516, despite the differences in metal content. The expected influence of metallicity on the coronal emission in this spectral range is complex as pointed out by Pizzolato et al. (2001). A first, direct effect is due to the radiative losses in the corona: the X-ray coronal spectrum of late type stars, at temperatures of a few million degrees, is dominated by line emission produced by heavy ions so that the emissivity power scales linearly with metal abundance.

A second effect is related to the structural change in subphotospheric layers due to the variation in metal abundance level. In fact, a higher metallicity increases the opacity and produces deeper convection zones at a given mass. This could result in a better efficiency of the dynamo, producing a higher coronal activity, if the rotational period is kept fixed. These two effects are likely to lead to an enhancement of X-ray coronal emission. Another effect is related to the metallicity influence on the mass vs. color-index relation: stars with higher metallicity at a fixed $B - V$ value are more massive than metal-poor stars with the same $B - V$. This effect produces variations in the convective turnover time of F−G type stars of up to a factor 4, if modeled with the Full-Spectrum-of-Turbulence theory (Canuto et al. 1996). A lower convective turnover time would imply a lower activity in metal-rich solar type stars with respect to metal-poor stars with the same color index because the compared stars have different masses. More massive metal-rich stars should have less extended convection zones and a less efficient dynamo mechanism than metal-poor stars with the same color index.

As a result, when we compare dG stars with different metal abundances selected by the same $B - V$ color index, the effects on the convection zone and on the radiative losses tend to compensate; for dK stars no effects on the convection zone are expected to be present and only the radiative losses are affected by metal abundance (Pizzolato et al. 2001).

The XLD for dK stars of Blanco 1 is similar to that of the Pleiades (Fig. 11), whereas based on the Pizzolato et al. (2001) model estimates, we would expect a monotonic increase of activity level with metal abundance. Two hypotheses are possible: either the presence of contaminating less active field stars lowers the overall distribution of $\log L_X$ (but the threshold of

---

[2] In Paper I the XLD of dG stars was marginally lower than that of Pleiades, in the present work this difference is not confirmed.
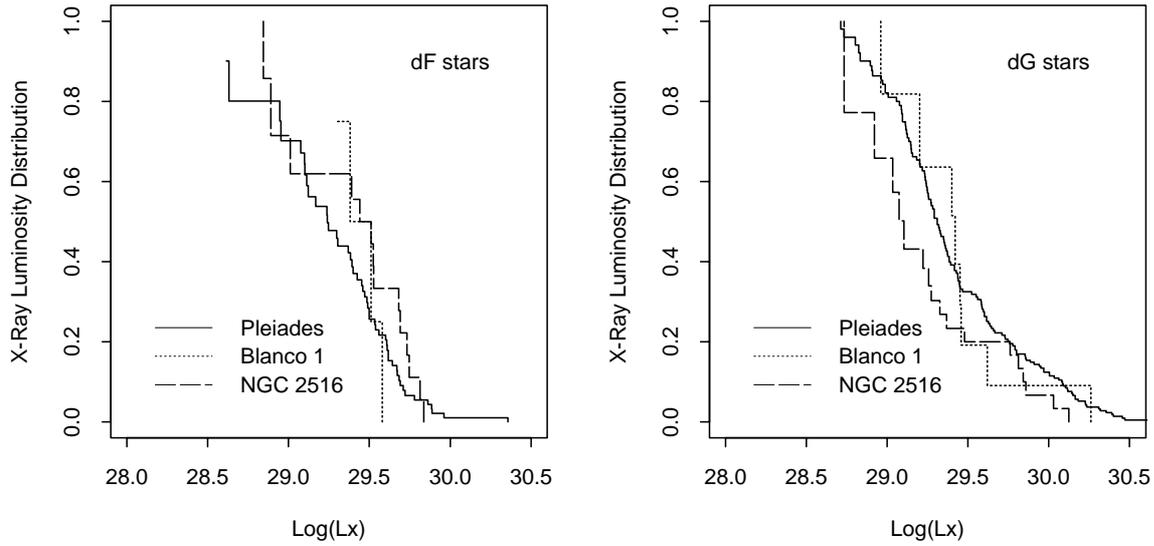
Fig. 10. XLDs for dF and dG stars of Blanco 1 (dotted line), Pleiades (continuous line) and NGC 2516 (dashed line).

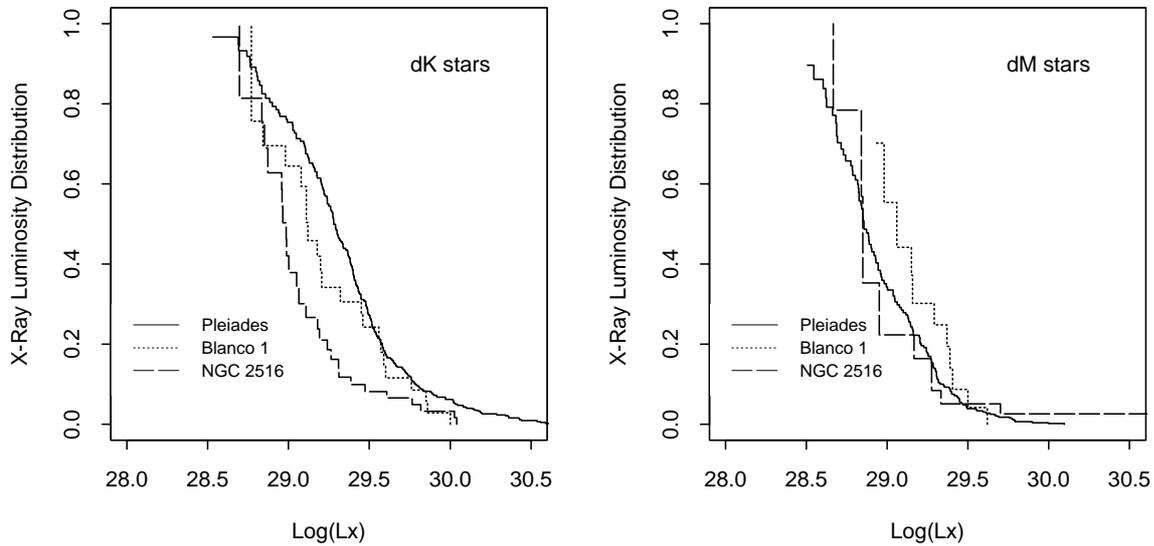
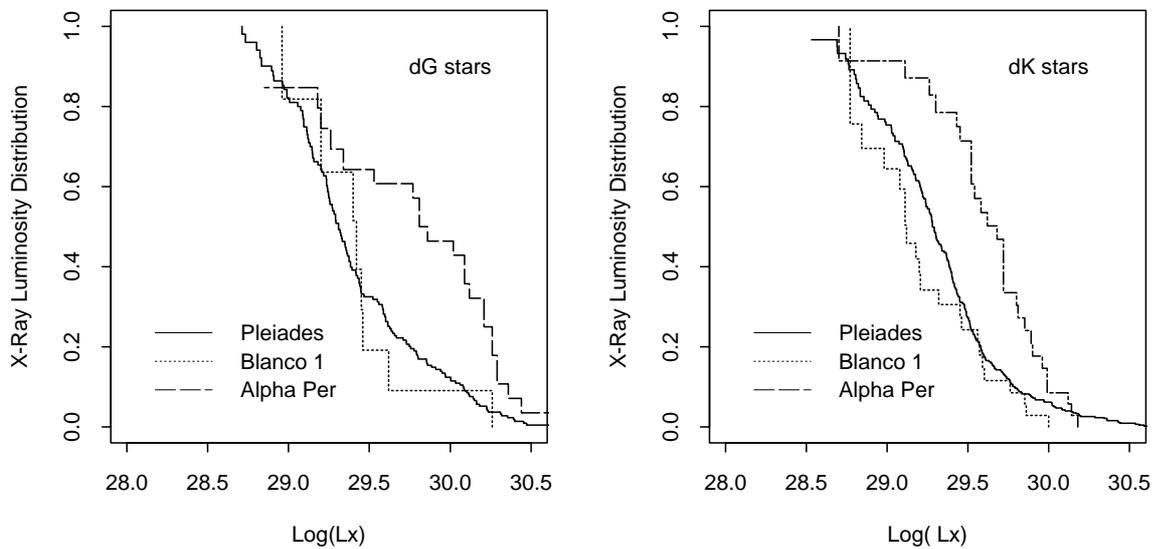**Fig. 11.** XLDs for dK and dM stars of Blanco 1 (dotted line), Pleiades (continuous line) and NGC 2516 (dashed line).

Fig. 12. XLDs for dG and dK stars of Blanco 1 (dotted line), Pleiades (continuous line) and α Per (dashed line).

membership probability is high enough to minimize this effect), or we are dealing with a real effect. In particular, a distribution of rotational periods different from that of Pleiades and NGC 2516 could overwhelm the metallicity effect in determining X-ray activity.

Measurements of $v \sin i$ are given in Jeffries & James (1999) for Blanco 1 G and K type stars selected from the list of Panagi & O'Dell (1997) and filtered by means of radial velocity criteria. The sample of members is very small but we note that the fraction of fast rotators is consistent with that found in the Pleiades by Queloz et al. (1998). These stars should be in the saturated coronal regime and this fact is consistent with the similarity of the high luminosity tails of XLDs of dK stars in Pleiades and Blanco 1, so that differences are to be looked for in the low velocity range (e.g. $v \sin i \leq 20$ km s^{-1}). The lack of measurements in this range for an extended sample of dK stars of Blanco 1 prevents us from testing for significant differences in the distributions of rotational periods.

For dM stars we note the relatively higher level of X-ray luminosity for the Blanco 1 sample. Whereas the distributions of Pleiades and NGC 2516 are similar, the XLD of Blanco 1 systematically presents higher values, although the high-luminosity tail is similar to that of the other clusters. This can suggest a possible metallicity effect on the X-ray emission of these stars. If we assume that the expected fraction of contaminants (∼10%) is concentrated in the lowest X-ray luminosity sources, we can correct the XLD, excluding the 10% of less active stars and obtaining the "non-contaminated" XLD. With this procedure we find that the probability level of a significant difference between the XLD of dM stars in Blanco 1 and Pleiades increases to 99.8%, thus reinforcing the indication that the chemical abundances are likely to play a role in the coronae of dM stars.

In Figs. 12 and 13 we compare the XLDs of Blanco 1, Pleiades and α Per to explore the effects related to age evolution. We note that in the case of dG and dK stars, the α Per stars are more X-ray luminous than those of Pleiades and Blanco 1. The dM stars of Blanco 1 appear, on the contrary, more X-ray luminous than those of Pleiades and α Per. It appears that the age effect on the X-ray emission level is relevant in the case of dG and dK stars while in the case of dM stars the differences in the Blanco 1 sample could be related to a metallicity effect.

We give some caveats on this conclusion: the Blanco 1 dM sample contains a small number of objects and the XLD is significantly influenced by upper limits. Deeper observations already planned with *XMM-Newton* satellite will allow us to give a firmer basis to this evidence.

4. Conclusions

We have calculated X-ray Luminosity Distributions for the Blanco 1 cluster from ROSAT-HRI data, taking advantage of a new astrometric-photometric membership selection. In particular we have calculated for the first time the XLD of Blanco 1 dM stars. Spatial cross-correlation between the GSC-II catalog and unidentified X-ray sources reported in Paper I allows us to identify new low-mass members characterized by high X-ray luminosity. We have also rejected a significant fraction of
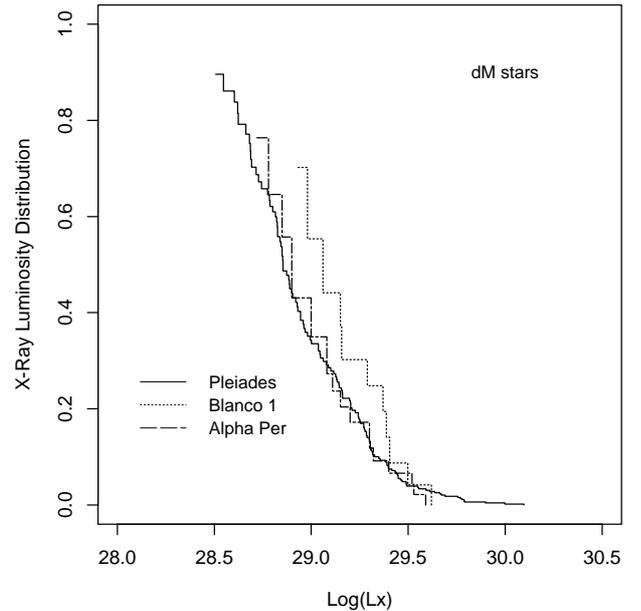
Fig. 13. XLDs for dM stars of Blanco 1 (dotted line), Pleiades (continuous line) and α Per (dashed line).

objects from the photometric member list of Panagi & O'Dell (1997), as having proper motions not compatible with those of the cluster.

The comparison of the new "uncontaminated" XLDs with the analogs of other clusters, allows us to explore effects related to age and metallicity, and shows that the metal-rich dM stars of Blanco 1 appear more active (with the caveats given in previous section) than the analog ones (more metal poor) in Pleiades, NGC 2516 and α Per. Our results suggest that chemical composition can influence coronal activity, mainly through coronal radiative losses due to emission lines. Deeper observations aimed to obtaining a larger sample of detections are needed to confirm these results based in part on upper limits.

The dK stars of Blanco 1 do not follow the prediction based on Pizzolato et al. (2001) according to which these stars should be more luminous than the dK stars in the Pleiades, thus suggesting a possible difference (not measured up to now) in the rotational velocity distribution of slow rotators with respect to the Pleiades. The testing of this hypothesis will require an observational campaign to derive rotational periods of "slowly" ($v \sin i \leq 20$ km s^{-1}) rotating Blanco 1 members.

Appendix A: Table of cluster members properties

Table A.1. Optical, infrared and X-ray band properties of Blanco 1 members in the combined fields of view of the two ROSAT-HRI observations. Identifiers in the first column are from de Epstein & Epstein (1985) (prefix ZS) or from Paper I, Table 4 (prefix BLX). Positions are taken from GSC-II catalog. The *prob* column report the astrometric membership probability.

Id.	RA (2000)	Dec (2000)	prob	$B-V$ mag	$J-H$ mag	$H-K$ mag	$T_{\rm eff}$ K	$M/M_\odot$	$\log L_{\rm X}$
	0:01:37.8	−29:57:28.3	0.87	1.53	–	–	–	–	≤29.57
ZS 35	0:01:39.8	−30:04:38.6	0.91	1.31	–	–	4100	0.67	29.85
ZS 58	0:01:46.5	−29:46:38.9	0.93	0.51	–	–	6220	1.30	29.82
	0:01:49.5	−30:15:12.1	0.87	0.66	–	–	3700	0.67	–
	0:01:52.6	−30:05:36.0	0.81	1.45	–	–	3480	0.51	≤28.80
ZS 37	0:01:53.4	−30:06:12.9	0.92	1.52	0.58	0.23	3360	0.25	29.29
ZS 38	0:01:54.4	−30:07:42.0	0.92	1.08	0.52	0.19	4520	0.80	29.86
	0:01:54.5	−30:10:38.3	0.91	1.35	–	–	4050	0.64	≤29.46
ZS 40	0:01:56.9	−30:12:08.0	0.93	1.42	0.63	0.16	3850	0.54	29.45
ZS 39	0:01:57.7	−30:09:28.8	0.94	0.12	–	–	9500	2.00	≤29.37
BLX 7	0:02:00.8	−29:59:17.6	0.89	0.75	0.41	0.12	5540	1.10	29.42
BLX 9	0:02:01.3	−29:57:55.3	0.88	1.48	–	–	–	–	29.37
ZS 43	0:02:03.7	−30:10:25.1	0.91	1.57	0.66	0.18	3600	0.38	≤29.57
ZS 42	0:02:04.2	−30:10:34.5	0.92	1.29	0.53	0.19	4130	0.69	29.57
ZS 45	0:02:18.5	−29:51:08.6	0.92	0.65	–	–	5820	1.20	29.20
ZS 46	0:02:19.7	−29:56:07.6	0.90	1.20	–	–	4260	0.73	29.46
ZS 48	0:02:21.6	−30:08:21.7	0.93	0.27	–	–	8000	1.70	29.85
	0:02:24.3	−30:06:02.9	0.90	1.44	–	–	3800	0.51	≤28.89
ZS 53	0:02:24.3	−30:09:09.0	0.87	1.56	0.64	0.16	3700	0.42	≤29.09
BLX17	0:02:25.9	−29:52:39.2	0.92	1.45	0.63	0.22	3480	0.28	29.08
ZS 54	0:02:28.2	−30:04:43.6	0.88	0.96	0.43	0.21	4740	0.87	29.76
ZS 52	0:02:30.9	−30:17:02.0	0.90	1.59	0.63	0.19	3560	0.35	29.62
ZS 61	0:02:34.8	−30:05:25.6	0.93	0.84	0.55	0.09	5160	0.98	30.00
ZS 62	0:02:35.4	−30:07:02.0	0.92	0.61	0.40	0.06	5920	1.20	29.46
BLX24	0:02:48.4	−29:53:53.8	0.94	1.56	0.63	0.24	3710	0.23	29.06
BLX26	0:02:51.5	−29:54:49.3	0.90	1.53	0.74	0.19	3560	0.35	29.15
	0:02:52.2	−29:47:00.9	0.88	1.47	0.69	0.16	3700	0.43	≤29.27
BLX27	0:02:54.2	−30:06:55.9	0.85	1.46	0.51	0.28	3130	0.15	29.21
ZS 76	0:02:56.4	−30:04:45.1	0.93	0.76	–	–	5470	1.10	30.26
ZS 75	0:03:00.3	−30:03:21.8	0.93	0.76	0.52	0.08	5480	1.10	29.62
BLX34	0:03:00.5	−30:15:44.1	0.90	1.55	–	–	–	–	29.40
ZS 71	0:03:02.9	−29:47:44.2	0.92	1.41	0.73	0.19	3850	0.57	29.56
ZS 83	0:03:07.1	−30:15:17.4	0.86	0.75	–	–	5540	1.10	29.40
	0:03:07.8	−30:18:59.2	0.83	1.48	–	–	–	0.40	–
ZS 84	0:03:10.8	−30:10:49.1	0.92	0.50	0.25	0.05	6270	1.40	29.58
BLX37	0:03:11.5	−29:58:10.2	0.89	1.50	–	–	–	–	29.16
ZS 95	0:03:16.5	−29:58:47.7	0.93	0.75	–	–	5530	1.10	28.96
ZS 91	0:03:20.6	−29:49:22.9	0.94	0.43	0.21	0.10	6490	1.40	29.51
	0:03:20.8	−29:51:52.8	0.85	1.34	0.59	0.13	4050	0.64	≤29.10
ZS 96	0:03:21.8	−30:01:10.8	0.93	0.24	–	–	8000	1.80	29.54
	0:03:22.5	−29:51:52.8	0.80	1.42	0.50	0.32	–	0.55	≤29.44
ZS 94	0:03:24.2	−29:56:23.1	0.86	1.43	0.66	0.08	3880	0.53	28.77
ZS 90	0:03:24.4	−29:48:49.6	0.93	0.30	–	–	7200	1.70	29.61
ZS 93	0:03:24.7	−29:55:14.9	0.87	0.94	–	–	4790	0.88	29.32

Table A.1. continued.

Id.	RA (2000)	Dec (2000)	prob	$B-V$ mag	$J-H$ mag	$H-K$ mag	T_{eff} K	$M/M_\odot$	$\log L_X$
ZS104	0:03:31.9	−29:43:04.9	0.90	0.16	–	–	8400	1.90	29.79
	0:03:33.7	−30:15:44.2	0.88	0.60	–	–	6000	1.20	–
BLX46	0:03:34.5	−29:58:30.6	0.84	1.56	0.65	0.17	3650	0.39	29.39
	0:03:39.9	−29:58:45.0	0.93	1.40	0.63	0.23	3900	0.58	≤29.13
ZS107	0:03:50.2	−30:03:55.9	0.93	1.18	–	–	4300	0.75	≤29.34
ZS112	0:04:04.0	−29:58:26.7	0.92	0.76	0.42	0.15	5500	1.10	≤29.82
	0:04:09.2	−30:01:11.1	0.89	1.55	–	–	–	–	≤29.50
BLX50	0:04:25.8	−30:04:02.7	0.93	1.52	0.64	0.21	3460	0.30	29.50
	0:04:27.4	−30:04:57.6	0.88	1.55	0.59	0.20	3510	0.33	≤29.45
ZS129	0:04:31.7	−30:14:41.9	0.93	0.46	–	–	6390	1.40	≤29.59
	0:04:45.1	−30:05:20.2	0.87	1.48	–	–	–	–	≤29.19
ZS134	0:04:49.2	−30:00:53.2	0.93	0.84	–	–	5140	0.97	≤29.82
BLX56	0:04:52.5	−30:11:28.3	0.93	1.44	0.71	0.21	3800	0.51	29.11
BLX57	0:04:56.1	−30:06:53.0	0.92	1.39	0.68	0.23	3800	0.60	29.20
ZS138	0:04:58.8	−30:09:41.8	0.91	0.38	–	–	6740	1.50	29.38
BLX59	0:05:02.6	−30:07:33.3	0.93	1.45	0.58	0.25	3700	0.50	28.86
	0:05:02.8	−30:20:26.2	0.93	1.57	–	–	–	–	≤29.43
ZS144	0:05:07.1	−29:59:25.8	0.91	1.33	–	–	4060	0.65	29.59
	0:05:07.7	−30:20:00.7	0.81	1.52	–	–	–	–	≤29.62
BLX64	0:05:08.4	−30:04:07.1	0.90	1.42	0.60	0.27	3850	0.55	29.12
BLX66	0:05:10.9	−30:03:41.1	0.92	1.43	0.65	0.27	3880	0.53	28.84
	0:05:11.8	−29:58:34.2	0.91	1.57	0.55	0.35	2800	–	≤29.04
	0:05:12.7	−29:59:53.3	0.82	1.60	0.50	0.36	2750	–	≤28.93
ZS148	0:05:14.4	−29:54:24.0	0.90	0.51	–	–	6220	1.30	29.52
ZS147	0:05:17.5	−29:46:57.6	0.89	0.90	–	–	4940	0.90	≤29.84
ZS156	0:05:25.5	−30:18:35.6	0.93	1.29	–	–	4130	0.68	≤29.32
ZS161	0:05:26.8	−29:51:20.8	0.87	0.68	0.40	0.05	5780	1.20	≤29.43
ZS158	0:05:29.0	−30:08:32.2	0.94	1.09	–	–	4510	0.80	≤28.79
ZS160	0:05:30.9	−29:53:08.3	0.88	0.45	0.25	0.06	6400	1.40	≤29.30
ZS154	0:05:31.5	−30:20:51.7	0.92	0.93	–	–	4830	0.88	29.60
	0:05:33.4	−30:08:13.6	0.83	1.30	0.68	0.15	4110	0.68	≤28.82
	0:05:34.8	−29:51:47.0	0.93	1.46	–	–	–	–	≤29.38
ZS165	0:05:35.5	−29:57:06.6	0.92	0.79	0.48	0.04	5360	1.00	29.45
	0:05:37.6	−30:20:39.8	0.90	1.47	–	–	–	–	≤29.12
	0:05:38.9	−30:07:32.2	0.84	1.45	–	–	3480	0.51	≤29.28
	0:05:39.9	−30:17:08.8	0.90	1.52	–	–	–	–	≤29.19
	0:05:40.9	−30:13:55.3	0.89	1.50	–	–	–	–	≤28.96
ZS166	0:05:42.9	−29:57:38.9	0.91	0.13	–	–	–	–	≤28.99
	0:05:48.3	−30:16:56.8	0.87	1.62	–	–	–	–	≤29.14
ZS170	0:05:54.7	−30:06:26.0	0.92	0.56	–	–	6080	1.30	≤29.20
BLX79	0:05:58.1	−30:11:09.0	0.91	1.48	0.65	0.23	3360	0.25	28.98
ZS172	0:06:04.3	−30:02:11.9	0.88	1.43	0.61	0.28	3880	0.53	29.11
	0:06:10.8	−30:13:46.2	0.85	1.40	–	–	3900	0.59	≤29.18
ZS182	0:06:16.3	−30:05:57.3	0.93	0.50	–	–	6270	1.40	29.31
BLX84	0:06:17.7	−30:06:29.6	0.92	1.42	–	–	3850	0.56	29.18
	0:06:19.0	−30:22:22.7	0.90	0.75	–	–	5530	1.10	–
BLX88	0:06:34.0	−30:08:46.0	0.93	1.40	–	–	3900	0.58	29.29
	0:06:44.5	−29:54:35.4	0.84	1.48	–	–	3360	0.40	–
	0:06:57.7	−30:09:17.3	0.82	1.28	–	–	4140	0.69	≤29.70

References

Boesgaard, A. M., & Friel, E. D. 1990, ApJ, 351, 467

Canuto, V. M., Goldman, I., & Mazzitelli, I. 1996, ApJ, 473, 550

Damiani, F., Maggio, A., Micela, G., & Sciortino, S. 1997, ApJ, 483, 350

de Epstein, A. E. A., & Epstein, I. 1985, AJ, 90, 1211

Edvardsson, B., Pettersson, B., Kharrazi, M., & Westerlund, B. 1995, A&A, 293, 75

Epstein, I. 1968, AJ, 73, 556

Harnden, F. R. Jr., Adams, N. R., Damiani, F., et al. 2001, ApJ, 547, L141

Jeffries, R. D., & James, D. J. 1999, ApJ, 511, 218

Jeffries, R. D., Thurston, M. R., & Pye, J. P. 1997, MNRAS, 287, 350

Jones, B. 1997, Mem. Soc. Astron. It., 68, 833

Lang, K. R. 1992, Astrophysical Data I. Planets and Stars (Astrophysical Data I. Planets and Stars, X, 937 pp., 33 figs., Berlin: Springer-Verlag)

Leggett, S. K., Allard, F., Berriman, G., Dahn, C. C., & Hauschildt, P. H. 1996, ApJS, 104, 117

Leggett, S. K., Allard, F., & Hauschildt, P. H. 1998, ApJ, 509, 836

Mermilliod, J. C. 1981, A&A, 97, 235

Micela, G., Sciortino, S., Favata, F., Pallavicini, R., & Pye, J. 1999a, A&A, 344, 83

Micela, G., Sciortino, S., Harnden F. R. Jr., et al. 1999b, A&A, 341, 751

Micela, G., Sciortino, S., Kashyap, V., Harnden, F. R. Jr., & Rosner, R. 1996, ApJS, 102, 75

Panagi, P. M., & O'Dell, M. A. 1997, A&AS, 121, 213

Pizzolato, N., Ventura, P., D'Antona, et al. 2001, A&A, 373, 597

Queloz, D., Allain, S., Mermilliod, J., Bouvier, J., & Mayor, M. 1998, A&A, 335, 183

Raymond, J. C., & Smith, B. W. 1977, ApJS, 35, 419

Robichon, N., Arenou, F., Mermilliod, J., & Turon, C. 1999, A&A, 345, 471

Schmitt, J. H. M. M. 1985, ApJ, 293, 178

Siess, L., Dufour, E., & Forestini, M. 2000, A&A, 358, 593

Westerlund, B. E., Lundgren, K., Pettersson, B., Garnier, R., & Breysacher, J. 1988, A&AS, 76, 101